Design Considerations and Experimental Results of a 100 W, 500000 rpm Electrical Generator

C. Zwyssig and J. W. Kolar
Power Electronic Systems Laboratory
Swiss Federal Institute of Technology Zurich
Physikstrasse 3, 8092 Zurich, Switzerland
Tel +41-44-6322837, Email zwyssig@lem.ee.ethz.ch

Abstract

A 100 W, 500000 rpm high-speed permanent-magnet generator/starter for a gas turbine based portable power unit has been designed and constructed. This paper presents the main design considerations for the machine and experimental measurements of a test bench. The losses due to the high frequency operation are minimized by choosing an appropriate stator core material and using a litz wire winding. Measurements match the predictions from the design stage.

1. Introduction

The increasing need for high energy density portable power devices has led to intense research and development efforts on mesoscale systems with power outputs up to a hundred Watts [1]. In this power range traditional batteries are challenged by devices that use fuel since the fuel provides significantly higher chemical energy density. An especially promising way of converting the energy stored in the fuel into electrical energy is to use gas turbine generator sets. All power supply systems of this type require an electrical system consisting of a high-speed generator/starter, power electronics, a control platform and a form of energy storage to power the starting of the turbine. However, the research so far has only concentrated on the turbine design, and very little research effort has occurred on determining the requirements and the design of the electrical system. Therefore, this paper focuses on the design and experimental analysis of a high-speed generator with a rated speed of 500000 rpm and an electrical power output of 100 W. The main challenges of the generator design are the losses due to the high frequency in the stator core and windings, the bearing technology, the rotor dynamics and a rotor design minimizing mechanical stresses and eccentricity.

The flux density in an electrically excited motor decreases with decreasing size. In contrary, permanent-magnet flux density remains constant for decreasing machine volume. Therefore, a permanent-magnet machine is chosen with the aim for a low system volume. High-speed operation requires a simple and robust rotor geometry and construction, and excessive mechanical stresses can be limited with a small rotor diameter. Therefore, a radial-flux machine is chosen with a cylindrical permanent magnet encased in a retaining sleeve. A length-to-diameter ratio of 1:1 is defined. This leads to a short shaft which increases the critical speed. The machine designed has an active length of 15 mm and a stator diameter of 16 mm. For highest torque density, high-energy rare earth magnets such as sintered NdFeB or SmCo are the only choices. A Sm_2Co_{17} based magnet is chosen because of its outstanding thermal characteristics (operating temperatures up to 350 °C). A slotless winding is chosen in order to keep the rotor losses low and the stator core manufacturing simple [2]. The peak value of the back EMF is set to 16 V in order to allow the use of low on-resistance power MOSFETs in the power electronic converter. With this benchmark data the electromagnetic machine design is carried out with the help of the finite-element software FEMAG [3] for a rated power of 100 W at a speed of 500000 rpm. A cross section of the machine at the design stage can be seen in Figure 1.

2. Electrical Considerations

The permanent magnet has only two poles in order to keep the fundamental frequency low, nevertheless the frequency of the currents and the magnetic field in stator winding and core reaches 8.3 kHz at rated speed. This leads to high eddy-current and hysteresis losses, which have to be minimized.

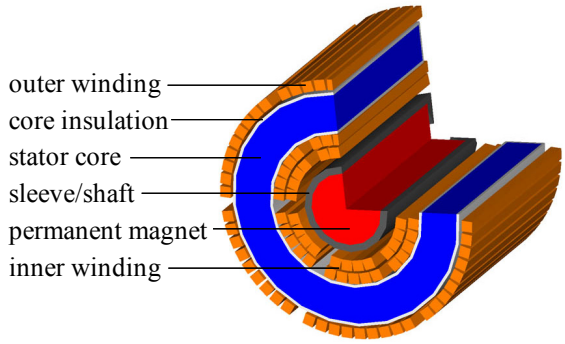

Figure 1. Cross section of the slotless brushless permanent-magnet generator with ring-wound stator. The rotor diameter is 6 mm, the stator core inner diameter is 11 mm, the stator core outer diameter is 16 mm and the active length is 15 mm.

2.1. Stator Winding Losses

Since the stator currents have a fundamental frequency of 8.3 kHz, the losses due to skin effect have to be taken into account. Furthermore, the active part of the winding is exposed to the magnetic field produced by the permanent magnet that rotates with the same frequency. This results in additional eddy current losses. These two losses can be calculated separately and then summed up [4]. For a single round wire the losses caused by the dc resistance and the skin effect are given by (2). The losses caused by the external magnetic field are independent of the current as can be seen from (3). The total losses $P_{tot} = P_s + P_p$ have a minimum for a certain diameter because (2) decreases and (3) increases with increasing diameter.

$$P_s = \frac{\hat{I}^2}{2} F \tag{2}$$

$$P_p = H_e^2 G \tag{3}$$

where $\hat{I}$ is the peak current and H_e the peak magnetic field strength, and the coefficients F and G are dependent on the conductor diameter, length, conductivity and frequency.

By using litz wire the current in each turn is divided into strands rather than flowing in a single conductor. For any number of strands, and a resulting current per strand, there exists an optimal strand diameter. With this optimal diameter, the total copper losses of the generator can be calculated for different number of strands (Figure 2). With the chosen litz wire of 60 strands and a diameter of 0.071 mm the losses are calculated to $P_{V,Cu} = 1.85$ W, which is a 70% reduction compared to using one conductor. The used area including isolation is $A_w = 7.5$ mm^2, which is still below the available winding area of $A_{w,a} = 8.3$ mm^2.

2.2. Stator Core Losses

In the stator core, the magnetic field rotates with high frequency (8.3 kHz) and therefore, a high frequency magnetic material is required. Possible choices are:

1. Silicon-iron, 168 µm laminations
2. Amorphous iron-based materials
3. Nanocrystalline iron-based materials
4. Ferrite
5. Nickel-iron, 100 µm laminations
6. Soft magnetic composites

For sinusoidal induction the core losses for most magnetic materials can be determined using the Steinmetz equation

$$P_{V,core} = C_m \cdot f^{\alpha} \cdot B_m^{\beta} \tag{4}$$

where C_m, α and β are taken from datasheets. For a first comparison of the materials, the stator core losses are calculated for a frequency of $f = 10$ kHz and a peak magnetic flux density of $B_m = 0.5$ T (Table 1).
Due to the lowest losses and the high Curie temperature nanocrystalline materials look very promising. However, currently only ring tape cores are manufactured. This is optimal for power inductors and transformers, where the magnetic flux flows along the core. But in the generator the magnetic flux lines enter the core in radial direction, which

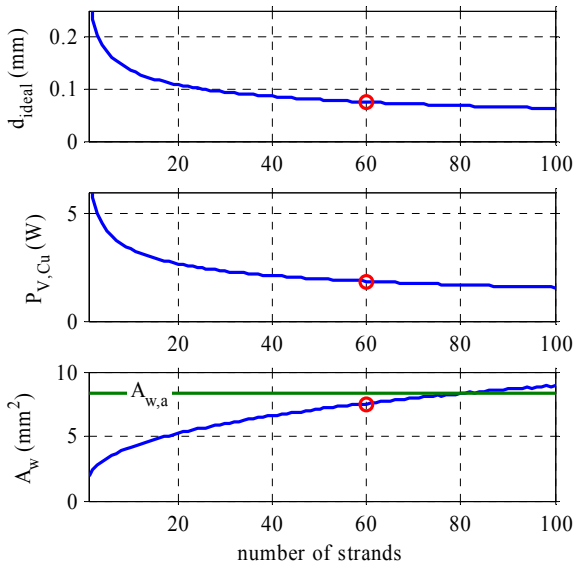

Figure 2. Ideal diameter of one strand (d_{ideal}), total generator copper losses ($P_{V,Cu}$) and resulting winding area (A_w) versus number of strands. A_w is calculated with a copper filling factor of 0.31. The available winding area is $A_{w,a} = 8.3$ mm^2. The average magnetic flux in the winding is $B = 0.32$ T at a frequency of 8.3 kHz.

Table 1. Core Material Properties

	Density (g/cm^3)	Curie temp. (°C)	Rel. perm. μ_r	Sat. B_{max} (T)	Losses[a] (W/cm^3)
1. Si-Fe	7.6	740	2000	1.7	3.5
2. Am.	7.29	358	<20000	1.41	0.15
3. Nanoc.	7.3	570	<70000	1.3	0.02
4. Ferrite	4.85	120	<15000	0.5	0.175
5. Ni-Fe	8.2	310	<80000	1.48	0.746
6. SMC	3.18	450	<500	2	2.8

a. Losses at a frequency of 10 kHz and a peak flux density of 0.5 T.

results in higher eddy current losses in the vicinity of the entering areas. In high-speed motors for the dental industry, mainly Ni-Fe is used as stator core material. As an example, in a Ni-Fe core with a volume of 1.6 cm^3, a peak flux density of 0.5 T and a frequency of 10 kHz, stator core losses of $P_{V,core} = 1.2$ W occur.

3. Mechanical Considerations

In contrary to the usual gluing of the magnets to the shaft, in this machine the retaining sleeve is shrink-fitted onto the permanent magnet and the fully assembled rotor is ground in order to minimize eccentricity without the need of balancing.

3.1. Mechanical Stresses

With an interference fit of rotor sleeve and permanent magnet, the stresses on the brittle magnet at high speed are

limited. But the stresses in the sleeve are already high at standstill and increase with speed. They can be calculated analytically according to [5]. The biggest stresses in the whole rotor occur on the inner side of the retaining sleeve. For a titanium alloy sleeve and interference fit of 15 µm the tangential stress σ_θ becomes 300 N/mm^2 at standstill and 325 N/mm^2 at rated speed (Fig. 3, Fig. 4). With the proper dimensioning of the interference fit the stresses in the magnet can be kept low and the stresses in the sleeve are a sufficient safety margin to the tensile strength of titanium (895 N/mm^2). With increasing speed the interference fit loosens due to the body load. The radial stress ($\sigma_{r,tit}=\sigma_{r,pm}$) must be negative (pressure) over the whole speed range in order to guarantee the torque transfer from the permanent magnet to the retaining sleeve, which also acts as shaft.

3.2. Critical Speeds

In order to run the machine in between two critical speeds, the bending modes of the rotor are determined with finite element simulations. The spring constant of the bearing system is taken into account, which shifts the bending modes to lower frequencies. The length of the shaft is adjusted such that rated speed (500000 rpm, 8333 Hz) falls between the second and the third bending modes (Table 2).

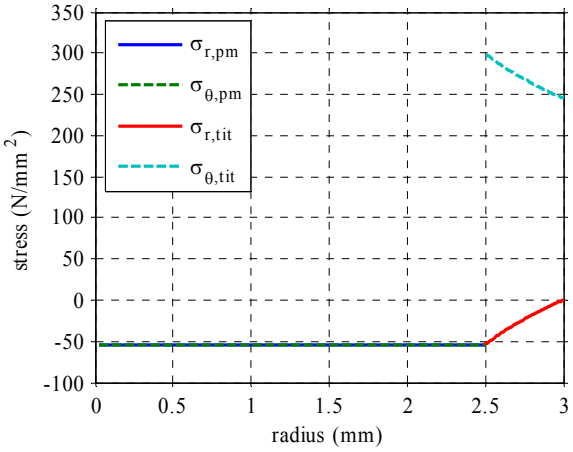

Figure 3. Stresses in Sm_2Co_{17} permanent magnet and titanium sleeve at standstill and a temperature of 23 °C and an interference fit of 15 µm.

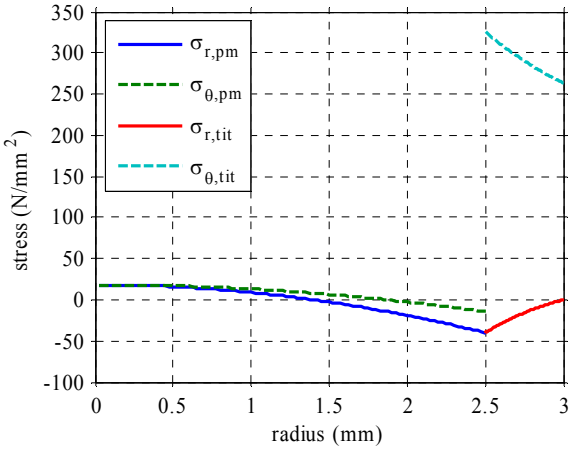

Figure 4. Stresses in Sm_2Co_{17} permanent magnet and titanium sleeve for a speed of 500000 rpm and a temperature of 23 °C and an interference fit of 15 µm.

4. Test Bench Setup

An experimental test bench is built in order to verify theoretical considerations and the generator concept. Two machines are arranged on a common shaft, one is operated as driving motor, and one as generator. The rotor is supported by two radial single row high-speed ball bearings and consists of a titanium retaining sleeve integrating two diametrically magnetized Sm_2Co_{17} permanent magnets, one for the motor and one for the generator. The stator is a ring-wound litz wire around a Ni-Fe core. Figure 5 shows a picture of the test bench setup. The torque is transformed with a moment arm into a force and then measured with a special piezoresistive sensor.

5. Measurements

With all the parts assembled in the test bench, the theoretical results are verified with initial measurements. The motor is driven open loop with an impressed three phase current of 2.5 A that is of adjustable frequency. For the first tests an impressed current with a frequency of 5 kHz is used to rotate the motor and generator at 300000 rpm. From the no-load test on the generator side a back EMF of 9.6 V peak is measured. Since the back EMF is proportional to the speed this matches the 16 V peak for 500000 rpm predicted by finite element analysis. As can be seen from Figure 6 the back EMF is

Table 2. Bending Modes

Sleeve material	Titanium	Steel
First bending mode	2400 Hz	2300 Hz
Second bending mode	4250 Hz	3730 Hz
Third bending mode	9880 Hz	9020 Hz

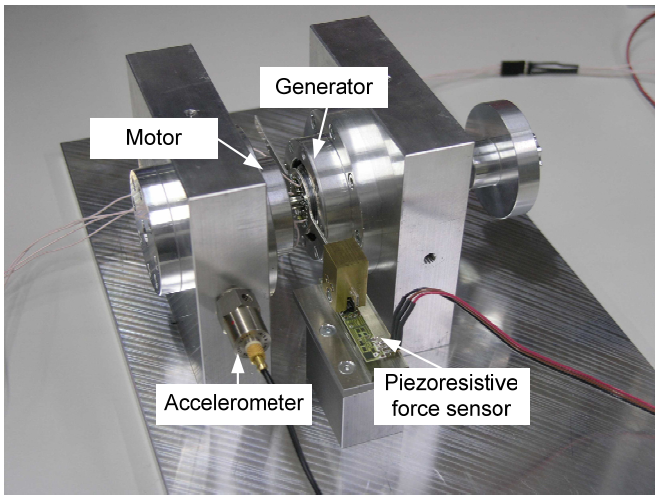

Figure 5. Photograph of the test bench showing motor, generator and sensors.

perfectly sinusoidal. An adjustable resistive three phase load is then connected to the generator side. The generator phase currents are varied between 0 and 2.2 A, the torque is measured and compared to the finite-element calculations. Again, there is a very good agreement between predictions and tests (Figure 7).

6. Future Steps

In order to drive the machine with the rated speed suitable power and control electronics are developed. A voltage source inverter with external inductances drives the permanent-magnet machine. The requirements on current control bandwidth are extremely high and the switching frequency exceeds 100 kHz. For a sensorless control a digital signal processor is used. Finally, the electronics should be small and lightweight. Figure 8 shows all the parts of the high-speed drive system.

7. Conclusion

A high-speed, 100 W, 500000 rpm permanent magnet generator design for mesoscale gas turbines has been presented in this paper. The losses in the copper winding due to the high frequency currents and magnetic field from the permanent magnet are calculated. The total copper losses are reduced by choosing an appropriate litz wire. To minimize the stator core losses different magnetic materials are compared and it is shown that amorphous and nanocrystalline materials are the best choices. The rotor is designed with a sufficient safety margin for the mechanical stresses. Titanium is used as retaining sleeve material in order to limit the stresses on the high-energy Sm_2Co_{17} magnets.
To verify the analytical calculations a test bench has been built, which consist of two machines (one acting as motor and one as generator) on a common shaft. The critical speeds for the test bench rotor are identified and the length of the shaft is adjusted such that rated speed falls between the second and the third bending modes. The measurements on the test bench of the back EMF and the torque match the values obtained by finite-element simulations very well. Further measurements will be carried out with custom-built power and control electronics for motor and generator.

References

[1] S. A. Jacobson and A. H. Epstein, "An informal survey of power mems," ISMME2003, Tsuchiura, Japan, December 1-3, 2003, pp. 513-520.

[2] N. Bianchi, S. Bolognani, and F. Luise, "Potentials and limits of high-speed pm motors," IEEE Trans. Industry Applications, vol. 40, no. 6, pp. 1570-1578, Nov.-Dec. 2004.

[3] K. Reichert, "A simplified approach to permanent magnet motor characteristics determination by finite-element methods", 16th International Conference on Electrical Machines ICEM, Cracow, Poland, September 5-8, 2004.

[4] J. A. Ferreira, Electromagnetic modeling of power electronic converters. Norwell, Massachusetts: Kluwer Academic Publishers, 1989, ch. 6.

[5] S. P. Timoshenko and J. N. Goodier, Theroy of elasticity. McGraw-Hill Kogakusha, Ltd. 1970, ch. 4.

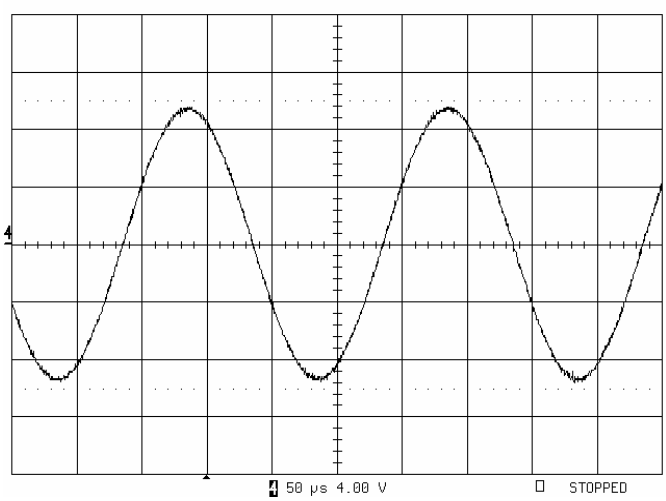

Figure 6. Measured back EMF of the generator in the test bench at 300000 rpm (50 µs/div, 4 V/div).

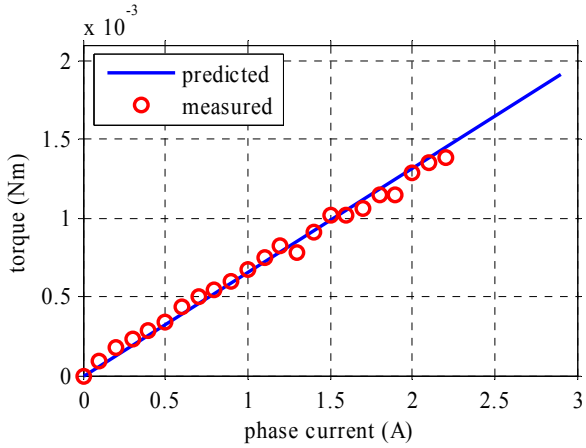

Figure 7. Comparison of predicted and measured torque over phase current.

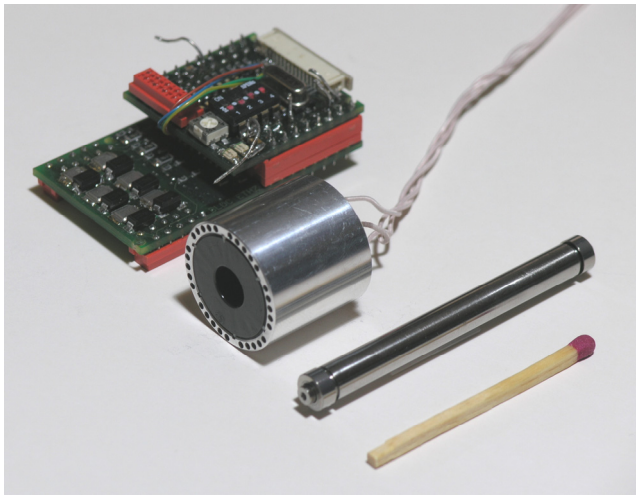

Figure 8. Power and control electronics, stator and rotor with assembled high-speed ball bearings.